THE JOURNAL OF PHYSICAL CHEMISTRY LETTERS
A JOURNAL OF THE AMERICAN CHEMICAL SOCIETY

pubs.acs.org/JPCL

Letter

Two-Dimensional Infrared Spectroscopy of Isolated Molecular Ions

Zifan Ma, Liangyi Chen, Chuzhi Xu, and Joseph A. Fournier*

Cite This: J. Phys. Chem. Lett. 2023, 14, 9683−9689

Read Online

ACCESS | Metrics & More | Article Recommendations | Supporting Information

ABSTRACT: Two-dimensional infrared (2D IR) spectroscopy of mass-selected, cryogenically cooled molecular ions is presented. Nonlinear response pathways, encoded in the time-domain photodissociation action response of weakly bound N_2 messenger tags, were isolated using pulse shaping techniques following excitation with four collinear ultrafast IR pulses. 2D IR spectra of $Re(CO)_3(CH_3CN)_3^+$ ions capture off-diagonal cross-peak bleach signals between the asymmetric and symmetric carbonyl stretching transitions. These cross peaks display intensity variations as a function of pump−probe delay time due to coherent coupling between the vibrational modes. Well-resolved 2D IR features in the congested fingerprint region of protonated caffeine ($C_8H_{10}N_4O_2H^+$) are also reported. Importantly, intense cross-peak signals were observed at 3 ps waiting time, indicating that tag-loss dynamics are not competing with the measured nonlinear signals. These demonstrations pave the way for more precise studies of molecular interactions and dynamics that are not easily obtainable with current condensed-phase methodologies.

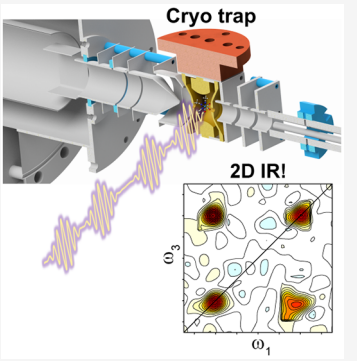

Downloaded via WASHINGTON UNIV on October 23, 2023 at 17:57:08 (UTC).
See https://pubs.acs.org/sharingguidelines for options on how to legitimately share published articles.

There has been an impressive growth of experiments adapting condensed-phase ultrafast nonlinear spectroscopic methodologies for the study of molecular systems isolated in the gas phase.[1−13] Ultrafast transient and multidimensional spectroscopies provide a wealth of structural and dynamical information not easily obtained from linear spectra, such as energy transfer and relaxation dynamics, frequency correlation dynamics, orientational dynamics, and intramolecular/intermolecular interactions encoded through off-diagonal cross-peak features.[14,15] Acquisition of well-resolved nonlinear spectra of gaseous species in a controlled environment, free from solvent effects, thermal broadening, and other sources of congestion, has the potential to uncover new fundamental insights into molecular interactions and dynamics that are not currently accessible with condensed-phase methodologies. Data from such gas-phase experiments would also provide stringent benchmarks for computational predictions and aid in the interpretation of complementary condensed-phase experiments.

The merger of mass spectrometric ion processing techniques with nonlinear ultrafast spectroscopies is particularly enticing.[16−22] Soft ionization techniques such as electrospray ionization enable the extraction of complex and diverse chemical, biological, and nanomaterial systems into the gas phase from nM−μM solutions. Extracted ions can be further processed to controllably produce the desired chemical species, for example, through H−D exchange, generation of reactive intermediates, or clustering with solvent molecules.[23,24] Buffer gas cooling in cryogenic ion traps offers additional advantages by quenching molecular systems into their lowest-energy configurations. Critically, spectroscopic analyses can be performed on the precise composition-selected system of interest.

A major drawback of spectroscopic studies on gaseous ions is the low number density ($<10^6$ cm^{-3}) that can be stored in ion traps. Consequently, the direct measurement of light absorption or an emitted nonlinear signal field is not feasible. Indirect "action" responses that encode light−matter interactions must instead be measured. In the widely used messenger tagging approach,[25] the parent ion is complexed with weakly bound "tag" molecules (He, H_2, N_2, Ar). These complexes only form under supersonic expansion conditions or under cryogenic buffer gas cooling in an ion trap. In standard frequency-domain experiments, a high-resolution laser source (typically few to sub-cm^{-1} resolution, nanosecond pulse duration) is frequency scanned through the optical region of interest. Resonant excitation of the parent ion results in photodissociation of the tag molecule through intramolecular vibrational redistribution (IVR) of the excitation energy[26] in the single-photon regime. Measurement of the photodissociation yield as a function of the laser frequency generates an action spectrum. As long as the tag binding energy is below the laser photon energy, the resulting action spectrum is directly proportional to the linear optical spectrum of the parent ion.

The application of ultrafast pulses also presents the challenge of how to frequency resolve an action response

Received: September 21, 2023
Revised: October 17, 2023
Accepted: October 19, 2023

© XXXX American Chemical Society

https://doi.org/10.1021/acs.jpclett.3c02661
J. Phys. Chem. Lett. 2023, 14, 9683−9689

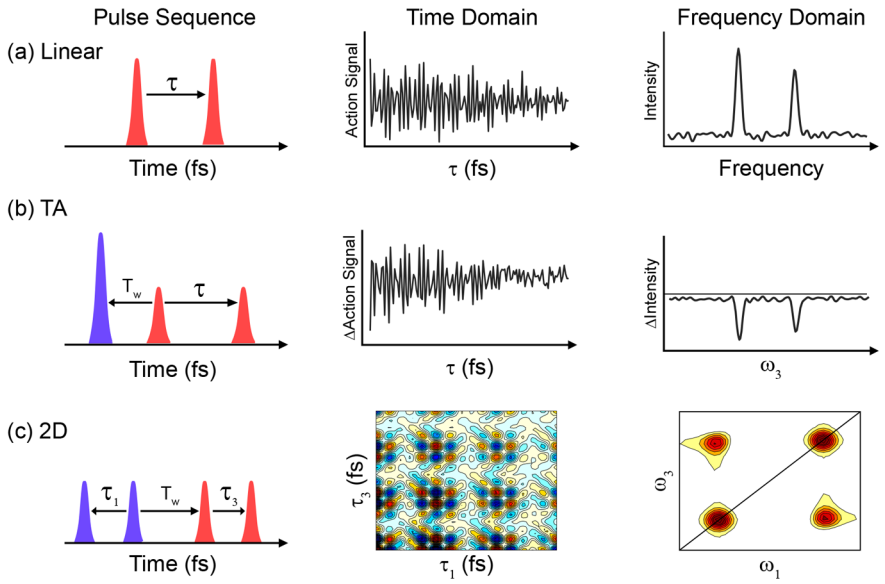

Figure 1. Hierarchy of frequency-resolved, action-detected spectroscopies using ultrafast light pulses. The respective pulse sequences, measured time-domain action signals, and processed frequency-domain spectra are illustrated. (a) Linear spectra are collected by monitoring the action response as a function of the delay time τ between a pulse pair. (b) Transient absorption (TA) spectra utilize a pump pulse preceding a probe pulse pair by a waiting time T_w. The action signal is monitored as a function of the probe pair delay time τ. (c) Two-dimensional (2D) spectra are collected as a function of the delays between a pump pair (τ_1) and probe pair (τ_3). A 2D-Fourier transform resolves the pump (ω_1) and probe (ω_3) frequency axes.

with a broadband source. Seminal work by Marcus,[27−29] Brixner,[30,31] Stienkemeier,[32,33] and others[34−39] have established the ability of indirect action responses, such as fluorescence, ionization, and photofragmentation, to encode nonlinear molecular responses. These responses can be frequency-resolved from time-domain measurements collected using a series of pulses. Key to these experiments is the use of pulse shapers to precisely control the delays and, crucially, phases of each pulse.[40] Phase-cycling schemes can then be applied to create and isolate the desired nonlinear signals encoded in the action response.[41]

Motivated by these studies, we have worked toward the implementation of ultrafast, frequency-resolved transient absorption (TA) and two-dimensional (2D) cryogenic ion vibrational spectroscopy (CIVS). We previously demonstrated the acquisition of linear infrared spectra of cryogenically cooled ions using an ultrafast pulse pair (Figure 1a).[42] The tag-loss photodissociation signal oscillates as a function of the delay time, τ, between the pulses due to interferences between the excited vibrational coherences, with the Fourier transform yielding the frequency-domain linear action spectrum. More recently, we presented the acquisition of TA-CIVS where excitation by a pump pulse precedes a probe pulse pair (Figure 1b).[43] Data are again collected in the time domain as a function of the probe pair delay time to frequency resolve the probe (ω_3) axis. An eight-step phase-cycling scheme isolates the TA signal from background linear and double quantum pathways, allowing for the measurement of bleaching signals of the fundamental transitions that evolve with the pump−probe waiting time, T_w. Herein, we present the first 2D-CIVS spectra. Four collinear pulses, consisting of a pump pulse pair and a probe pulse pair, are used to excite tagged molecular ions (Figure 1c). The tag-loss action signal is monitored as a function of both the pump pair delay, τ_1, and the probe pair delay, τ_3, using a 27-step phase-cycling scheme. A 2D-Fourier transform of the time-domain data produces a 2D IR spectrum that is frequency-resolved along the pump (ω_1) and probe (ω_3) axes. Detailed descriptions of the experimental methodologies and data processing procedures are provided in the Supporting Information.

We first investigated the *fac*-$Re(CO)_3(CH_3CN)_3^+ \cdot N_2$ complex (Figure 2a) in the carbonyl stretch region. There are two features in the linear IR spectrum: a doubly degenerate asymmetric carbonyl stretch near 2000 cm^{-1} and a symmetric carbonyl stretch near 2080 cm^{-1} (top panel in Figure 2b). The bottom panel of Figure 2b presents the previously reported[43] TA-CIVS spectra at 200 and 400 fs waiting times, showing relatively strong bleaching signals at the two fundamental frequencies. Importantly, there are notable intensity differences between the two spectra. Our previous measurements[43] showed intensity modulations in both bleach signals with a period of ∼417 fs, matching the energy difference between the two transitions. The presence of such oscillations with pump−probe waiting time are indicative of strong coherent coupling between the vibrational modes.[14,44−46] The implied presence of mode coupling is expected to manifest as off-diagonal cross peaks between the asymmetric and symmetric carbonyl stretches in a 2D IR spectrum. 2D-CIVS spectra at 208 fs (TA minimum) and 417 fs (TA maximum) waiting times are presented in Figure 2c,d, respectively. Cross-peak features between the carbonyl stretch transitions are clearly recovered, in addition to the diagonal bleach signals. The cross peaks and overall signal are stronger at T_w = 417 fs compared to 208 fs, consistent with the TA spectra and reported solution-phase 2D IR spectra of metal carbonyl complexes.[47,48] Note that the 2D-CIVS spectra were collected in the ZZZZ polarization scheme (all pulses parallel). Since the asymmetric and symmetric carbonyl stretches have orthogonal transition moments, the cross-peak signal will be strongest in the ZZYY scheme. The 2D lineshapes, in general, appear homogeneously broadened

https://doi.org/10.1021/acs.jpclett.3c02661
J. Phys. Chem. Lett. 2023, 14, 9683−9689

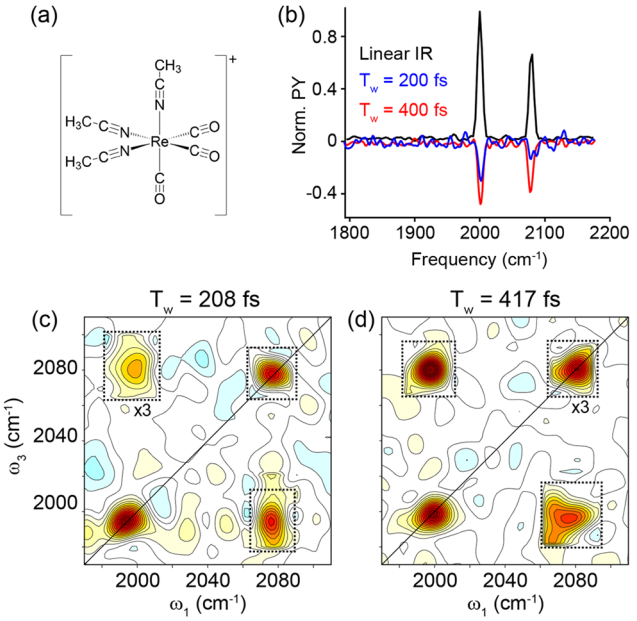

Figure 2. (a) Structure of *fac*-$Re(CO)_3(CH_3CN)_3^+$. (b) Linear and TA-CIVS spectra at 200 and 400 fs waiting times in the carbonyl stretch region. (c) 2D-CIVS spectrum at 208 fs waiting time (TA signal minimum). (d) 2D-CIVS spectrum at 417 fs waiting time (TA signal maximum). Off-diagonal cross-peak features are present between the coupled asymmetric and symmetric carbonyl stretch modes. The regions outlined by dashed boxes were enhanced by a factor of 3 for better visualization.

with little apparent inhomogeneous diagonal elongation. This is, perhaps, not too surprising given the dilute, solvent-free environment and cryogenic conditions.

To further demonstrate that the 2D-CIVS spectra indeed capture nonlinear response pathways, we take a more detailed look at the asymmetric stretch bleach feature at T_w = 417 fs in Figure 3. Lineshapes in 2D spectroscopies derive from both absorptive and dispersive components, leading to "phase twists" that contain positive and negative contributions.[14] In addition, nonlinear signals derive from so-called rephasing and nonrephasing pathways.[14] Rephasing (or photon echo) pathways are those where the coherences during τ_1 and τ_3 evolve in the opposite sense, with the signal proportional to $e^{-i\omega_{10}(\tau_3-\tau_1)}$. Nonrephasing pathways evolve as $e^{-i\omega_{10}(\tau_3+\tau_1)}$. Feynman diagrams illustrating these pathways are provided in the Supporting Information. Importantly, rephasing and nonrephasing signals produce lineshapes with opposite phase twists. Adding or simultaneously collecting the rephasing and nonrephasing signals produces purely absorptive lineshapes. The 27-step phase-cycling scheme allows the absorptive, rephasing, and nonrephasing signals to be isolated from the same data set,[41,49] the real components of which are presented in Figure 3a–c, respectively. The respective imaginary components are presented in the Supporting Information. The rephasing and nonrephasing spectra for both the real and imaginary components display the appropriate phase twists[14,49,50] due to positive (blue) and negative (red) contributions to the lineshapes. These comparisons unequivocally show that the measured tag-loss photodissociation signal encodes the desired nonlinear light–matter interaction pathways.

Conspicuously absent from the absorptive 2D-CIVS spectra are positive induced absorption peaks deriving from overtone (diagonal) and combination band (off-diagonal) transitions that are hallmarks of condensed-phase experiments. The absence of induced absorption transitions is a consequence of the action-detection scheme. Conventional condensed-phase experiments measure the third-order macroscopic polarization of the system following interactions with the pump (two interactions) and probe (one interaction) pulses, which generates an emitted signal field that is directly detected following the probe interaction. Action-based methods are formally fourth-order experiments in which the measured action signal is directly proportional to the final excited-state population that causes the action following the second probe interaction (fourth interaction overall). Although even-order experiments generate no molecular response (macroscopic polarization) in isotropic media, the fourth-order population in an action experiment is a measurable quantity. This important difference results in a unique set of light–matter interaction pathways in action-detection experiments,[30,51] the Feynman diagrams for which are given in the Supporting Information. While action experiments result in pathways analogous to the third-order ground-state bleach, stimulated emission, and induced absorption pathways, there is an additional excited-state pathway that is not accessible in third-order experiments. This new pathway, which corresponds to a bleach of the excited state, destructively interferes with the induced absorption pathway. As a result, only bleaching signals are expected in action-based TA and 2D spectra.[27,30]

Although important molecular and dynamical information provided by induced absorption transitions are unavailable, the presence of bleach/induced absorption peak pairs in condensed-phase measurements often leads to significant spectral congestion in 2D IR spectra. This is particularly true

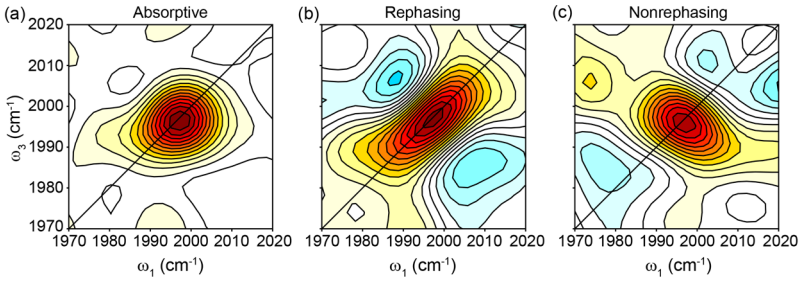

Figure 3. (a) Absorptive, (b) rephasing, and (c) nonrephasing signals of the asymmetric carbonyl stretch in *fac*-$Re(CO)_3(CH_3CN)_3^+$ at T_w = 417 fs shown in Figure 2d isolated through phase cycling. The rephasing and nonrephasing signals illustrate the expected phase twists due to contributions from absorptive and dispersive lineshape components.

https://doi.org/10.1021/acs.jpclett.3c02661
J. Phys. Chem. Lett. 2023, 14, 9683–9689

for large molecules, such as peptides, in the important fingerprint region. The lack of induced absorption features, along with the much sharper spectral transitions generally obtained with CIVS, could greatly aid in the interpretation of 2D spectra. As an example, the 2D-CIVS spectrum of protonated caffeine ($C_8H_{10}N_4O_2H^+$) in the 1650−1850 cm^{-1} region is presented in Figure 4. The linear spectrum is given in

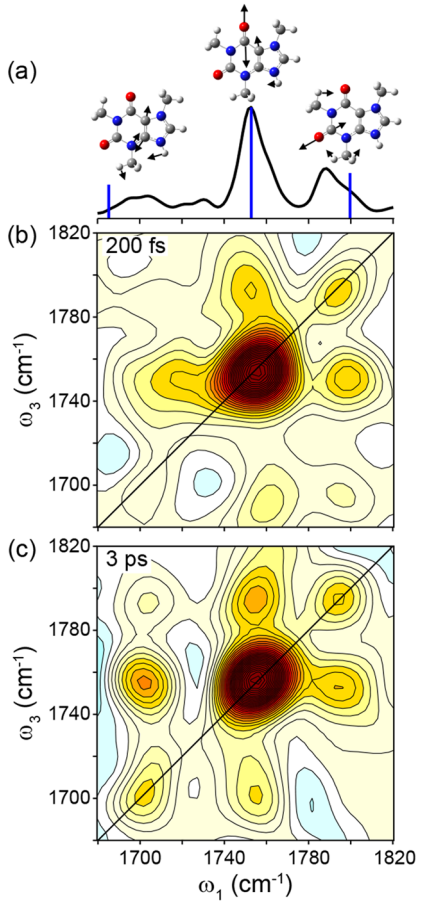

Figure 4. (a) Linear IR spectrum of protonated caffeine with calculated (B3LYP/6-311G(d,p), scaled by 0.99) stick spectrum and displacement vectors in the carbonyl stretch region. (b) 2D-CIVS spectrum at 200 fs waiting time. (c) 2D-CIVS spectrum at a 3 ps waiting time. The 2D spectra display distinct cross peaks between the three main transitions. The spectrum at 3 ps shows slightly stronger cross-peak signatures.

Figure 4a along with the calculated[52] stick spectrum. There are three closely spaced transitions: the stretching modes of the two carbonyl groups and a mixed NH^+ bending/CN stretching mode. Note that the two carbonyl stretches in neutral caffeine produce an asymmetric/symmetric stretch normal mode pair that results in strong 2D IR cross-peak signals in solution.[53] The calculated displacement vectors shown in Figure 4a, however, indicate that protonation acts to largely decouple the carbonyl stretch transitions. The NH^+ bend/CN stretch normal mode also appears mostly isolated from the carbonyl stretches. Despite the expectation of weaker coupling compared to neutral caffeine, the 2D-CIVS spectrum of protonated caffeine reveals relatively strong cross-peak signals between all three transitions at both 200 fs (Figure 4b) and 3 ps (Figure 4c) waiting times. This observation indicates the presence of anharmonic coupling between the three transitions, not unlike the coupling observed in condensed-phase 2D IR between amide I (CO stretch) and amide II (NH bend/CN stretch) modes in peptides.[54−56] Importantly, all 2D bleach features are well-resolved and free from significant spectral overlap and lineshape distortions. Further, the relatively high-quality spectra obtained from the weaker fingerprint C═O carbonyl stretching and NH^+ bending transitions in protonated caffeine compared to the much more intense C≡O carbonyl stretches in the metal carbonyl complex demonstrate the generality of the 2D-CIVS method.

A critical question regarding TA and 2D-CIVS is whether tag-loss dynamics interfere in the measurement of the desired nonlinear signals of the underlying parent ion. The strong cross peaks observed at 3 ps waiting time in Figure 4c indicate that tag-loss dynamics are not yet affecting the measurements. If tag loss occurs during the pump−probe waiting time period, the experiment becomes analogous to hole-burning: the pump acts to deplete the tagged ion population, causing less action signal to be produced by the probe. This would then result in static bleach signals along the diagonal and, importantly, no cross-peak signals. It is evident that this is not the case for protonated caffeine. Instead, both intramolecular and intermolecular vibrational relaxation processes appear to occur on relatively long time scales. Solution-phase studies on neutral caffeine measured ∼800 fs IVR time scales for the carbonyl stretches with a small solvent dependence.[53] While it is difficult to make quantitative conclusions at the current level of experimental uncertainty, the cross peaks qualitatively appear stronger and more distinct at 3 ps compared to 200 fs, suggesting vibrational energy transfer dynamics between the three modes. Intermolecular relaxation to solvent in neutral caffeine, on the other hand, was measured to occur on ∼5 ps (D_2O) and ∼10 ps (CH_3CN) time scales, respectively.[53] Intermolecular relaxation in isolated, cryogenically cooled protonated caffeine to a weakly interacting N_2 tag molecule, therefore, likely takes place on time scales ≫10 ps. Similarly, the oscillatory intensity modulations measured in our previous TA-CIVS experiments on *fac*-$Re(CO)_3(CH_3CN)_3^+$ persisted beyond 3 ps waiting time.[43] While not completely general, we posit that intermolecular vibrational relaxation to weakly bound tag molecules and subsequent tag-loss dynamics will, in most cases, take place on time scales much longer than the dynamics of interest for cryogenically cooled molecular ions.

With these successful demonstrations, we envision 2D-CIVS to be a powerful tool for structure determination and the study of intramolecular and intermolecular interactions through the recovery of well-resolved off-diagonal cross peaks. For example, the amide I and amide II spectral regions in peptides are highly congested and difficult to resolve at the amino acid level with condensed-phase 2D IR without the use of isotopic labeling.[57−59] While traditional CIVS affords higher frequency resolution (linewidths typically 5−10 cm^{-1}), experiments on small peptide systems usually require comparisons to computational predictions of many conformers and/or isomer-specific double resonance experiments to make structural identifications.[60−65] Well-resolved cross peaks across the amide I and II regions with 2D-CIVS will help guide conformational searches and provide less ambiguity in structural assignments. Another intriguing example would be the study of biomolecule−water interactions. Solvation shell interactions are incredibly difficult to study with condensed-phase 2D IR due to the overwhelming background water signal and bulk water's rapid vibrational dynamics.[66,67] Well-established clustering techni-

https://doi.org/10.1021/acs.jpclett.3c02661
J. Phys. Chem. Lett. 2023, 14, 9683−9689

ques[68−73] can be used to study biomolecule−water interactions one water molecule at a time. For peptides, ultrafast pulses provide sufficient bandwidth to interrogate the amide I, amide II, and water bending transitions simultaneously. Therefore, biomolecule−water cross peaks would directly report on the water binding sites.

Pulse shaping can alternatively be used to collect spectra more rapidly in the frequency domain using few cm^{-1} (few ps) bandwidth pump and/or probe pulses if subpicosecond dynamics are not critical. Ultrafast time resolution would be required for the study of strongly H-bonded systems, where H-bonded OH or NH groups often display surprisingly broad transitions even under cryogenic conditions.[74−77] This spectral breadth is predicted to arise from strong anharmonic coupling to lower-frequency modes, which results in rapid relaxation dynamics of the excited OH/NH stretch.[78−83] TA and 2D-CIVS can be used to track vibrational energy relaxation pathways in these systems. Further, 2D-CIVS would be able to reveal homogeneous vs inhomogeneous contributions to broad OH/NH stretch lineshapes and track frequency−frequency correlation dynamics (spectral diffusion) as energy relaxes into low-frequency soft modes. Finally, vibrational dynamics on excited electronic states can be measured using UV/vis pump-IR probe TA-CIVS, providing an exciting possible avenue for the study of photoinduced reaction dynamics and mechanisms.

■ ASSOCIATED CONTENT

Supporting Information

The Supporting Information is available free of charge at https://pubs.acs.org/doi/10.1021/acs.jpclett.3c02661.

Experimental methods and data processing procedures; imaginary rephasing, nonrephasing, and absorptive lineshapes; Feynman diagrams for 4th-order rephasing and nonrephasing pathways for uncoupled and coupled two-oscillator systems (PDF)

■ AUTHOR INFORMATION

Corresponding Author

Joseph A. Fournier − *Department of Chemistry, Washington University in St. Louis, St. Louis, Missouri 63130, United States;* orcid.org/0000-0001-7569-9176; Email: jfournier@wustl.edu

Authors

Zifan Ma − *Department of Chemistry, Washington University in St. Louis, St. Louis, Missouri 63130, United States*

Liangyi Chen − *Department of Chemistry, Washington University in St. Louis, St. Louis, Missouri 63130, United States;* orcid.org/0000-0002-9391-4332

Chuzhi Xu − *Department of Chemistry, Washington University in St. Louis, St. Louis, Missouri 63130, United States*

Complete contact information is available at: https://pubs.acs.org/10.1021/acs.jpclett.3c02661

Notes

The authors declare no competing financial interest.

■ ACKNOWLEDGMENTS

J.A.F. gratefully acknowledges support from NSF through a CAREER Award (Grant CHE-2044927).

■ REFERENCES

(1) Grimberg, B. I.; Lozovoy, V. V.; Dantus, M.; Mukamel, S. Ultrafast Nonlinear Spectroscopic Techniques in the Gas Phase and Their Density Matrix Representation. *J. Phys. Chem. A* **2002**, *106*, 697−718.

(2) Mandal, A.; Pack, G. N.; Shah, P. P.; Erramilli, S.; Ziegler, L. D. Ultrafast Two-Dimensional Infrared Spectroscopy of a Quasifree Rotor: J Scrambling and Perfectly Anticorrelated Cross Peaks. *Phys. Rev. Lett.* **2018**, *120*, No. 103401.

(3) Silfies, M. C.; Kowzan, G.; Lewis, N.; Allison, T. K. Broadband Cavity-Enhanced Ultrafast Spectroscopy. *Phys. Chem. Chem. Phys.* **2021**, *23*, 9743−9752.

(4) Daniels, D. A.; Wells, T. A.; Chen, P. C. High Resolution Two-Dimensional Infrared (HR-2DIR) Spectroscopy of Gas Phase Molecules. *J. Chem. Phys.* **2022**, *157*, No. 184201.

(5) Shipman, S. T.; Douglass, P. C.; Yoo, H. S.; Hinkle, C. E.; Mierzejewski, E. L.; Pate, B. H. Vibrational Dynamics of Carboxylic Acid Dimers in Gas and Dilute Solution. *Phys. Chem. Chem. Phys.* **2007**, *9*, 4572−4586.

(6) Schriever, C.; Lochbrunner, S.; Riedle, E.; Nesbitt, D. J. Ultrasensitive Ultraviolet-Visible 20 fs Absorption Spectroscopy of Low Vapor Pressure Molecules in the Gas Phase. *Rev. Sci. Instrum.* **2008**, *79*, No. 013107.

(7) Cole-Filipiak, N. C.; Troß, J.; Schrader, P.; McCaslin, L. M.; Ramasesha, K. Ultraviolet Photodissociation of Gas-Phase Iron Pentacarbonyl Probed with Ultrafast Infrared Spectroscopy. *J. Chem. Phys.* **2021**, *154*, No. 134308.

(8) Cole-Filipiak, N. C.; Troß, J.; Schrader, P.; McCaslin, L. M.; Ramasesha, K. Ultrafast Infrared Transient Absorption Spectroscopy of Gas-Phase $Ni(CO)_4$ Photodissociation at 261 nm. *J. Chem. Phys.* **2022**, *156*, No. 144306.

(9) Schnorr, K.; Belina, M.; Augustin, S.; Lindenblatt, H.; Liu, Y.; Meister, S.; Pfeifer, T.; Schmid, G.; Treusch, R.; Trost, F.; Slavíček, P.; Moshammer, R. Direct Tracking of Ultrafast Proton Transfer in Water Dimers. *Sci. Adv.* **2023**, *9*, No. eadg7864.

(10) Heald, L. F.; Gosman, R. S.; Rotteger, C. H.; Jarman, C. K.; Sayres, S. G. Nonadiabatic Photodissociation and Dehydrogenation Dynamics of n-Butyl Bromide Following p-Rydberg Excitation. *J. Phys. Chem. Lett.* **2023**, *14*, 6278−6285.

(11) Wolf, T. J. A.; Parrish, R. M.; Myhre, R. H.; Martínez, T. J.; Koch, H.; Gühr, M. Observation of Ultrafast Intersystem Crossing in Thymine by Extreme Ultraviolet Time-Resolved Photoelectron Spectroscopy. *J. Phys. Chem. A* **2019**, *123*, 6897−6903.

(12) Zettergren, H.; Domaracka, A.; Schlathölter, T.; Bolognesi, P.; Díaz-Tendero, S.; Łabuda, M.; Tosic, S.; Maclot, S.; Johnsson, P.; Steber, A.; Tikhonov, D.; Castrovilli, M. C.; Avaldi, L.; Bari, S.; Milosavljević, A. R.; Palacios, A.; Faraji, S.; Piekarski, D. G.; Rousseau, P.; Ascenzi, D.; Romanzin, C.; Erdmann, E.; Alcamí, M.; Kopyra, J.; Limão-Vieira, P.; Kočišek, J.; Fedor, J.; Albertini, S.; Gatchell, M.; Cederquist, H.; Schmidt, H. T.; Gruber, E.; Andersen, L. H.; Heber, O.; Toker, Y.; Hansen, K.; Noble, J. A.; Jouvet, C.; Kjær, C.; Nielsen, S. B.; Carrascosa, E.; Bull, J.; Candian, A.; Petrignani, A. Roadmap on Dynamics of Molecules and Clusters in the Gas Phase. *Eur. Phys. J. D* **2021**, *75*, 152.

(13) Wang, E.; Kling, N. G.; LaForge, A. C.; Obaid, R.; Pathak, S.; Bhattacharyya, S.; Meister, S.; Trost, F.; Lindenblatt, H.; Schoch, P.; Kübel, M.; Pfeifer, T.; Rudenko, A.; Díaz-Tendero, S.; Martín, F.; Moshammer, R.; Rolles, D.; Berrah, N. Ultrafast Roaming Mechanisms in Ethanol Probed by Intense Extreme Ultraviolet Free-Electron Laser Radiation: Electron Transfer versus Proton Transfer. *J. Phys. Chem. Lett.* **2023**, *14*, 4372−4380.

(14) Hamm, P.; Zanni, M. *Concepts and Methods of 2D Infrared Spectroscopy*; Cambridge University Press: Cambridge, United Kingdom, 2011.

(15) Cho, M. Coherent Two-Dimensional Optical Spectroscopy. *Chem. Rev.* **2008**, *108*, 1331−1418.

(16) Veenstra, A. P.; Monzel, L.; Baksi, A.; Czekner, J.; Lebedkin, S.; Schneider, E. K.; Pradeep, T.; Unterreiner, A. N.; Kappes, M. M. Ultrafast Intersystem Crossing in Isolated $Ag_{29}(BDT)_{12}^{3-}$ Probed by

Time-Resolved Pump-Probe Photoelectron Spectroscopy. *J. Phys. Chem. Lett.* **2020**, *11*, 2675−2681.
(17) Bull, J. N.; West, C. W.; Anstöter, C. S.; da Silva, G.; Bieske, E. J.; Verlet, J. R. Ultrafast Photoisomerisation of an Isolated Retinoid. *Phys. Chem. Chem. Phys.* **2019**, *21*, 10567−10579.
(18) Schüssler, L.; Israil, R. G. E.; Hütchen, P.; Thiel, W. R.; Diller, R.; Riehn, C. Ultrafast Spectroscopy of Ru^{II} Polypyridine Complexes in the Gas Phase and the Liquid Phase: $[Ru(2,2'\text{-bipyridine})_2(\text{nicotinamide})_2]^{2+}$. *Phys. Chem. Chem. Phys.* **2023**, *25*, 4899−4914.
(19) Gruber, E.; Kabylda, A. M.; Nielsen, M. B.; Rasmussen, A. P.; Teiwes, R.; Kusochek, P. A.; Bochenkova, A. V.; Andersen, L. H. Light Driven Ultrafast Bioinspired Molecular Motors: Steering and Accelerating Photoisomerization Dynamics of Retinal. *J. Am. Chem. Soc.* **2022**, *144*, 69−73.
(20) Guyon, L.; Tabarin, T.; Thuillier, B.; Antoine, R.; Broyer, M.; Boutou, V.; Wolf, J. P.; Dugourd, P. Femtosecond Pump-Probe Experiments on Trapped Flavin: Optical Control of Dissociation. *J. Chem. Phys.* **2008**, *128*, No. 075103.
(21) MacAleese, L.; Hermelin, S.; El Hage, K.; Chouzenoux, P.; Kulesza, A.; Antoine, R.; Bonacina, L.; Meuwly, M.; Wolf, J. P.; Dugourd, P. Sequential Proton Coupled Electron Transfer (PCET): Dynamics Observed Over 8 Orders of Magnitude in Time. *J. Am. Chem. Soc.* **2016**, *138*, 4401−4407.
(22) Marlton, S. J. P.; McKinnon, B. I.; Greißel, P.; Shiels, O. J.; Ucur, B.; Trevitt, A. J. Picosecond Excited-State Lifetimes of Protonated Indazole and Benzimidazole: The Role of the N-N Bond. *J. Chem. Phys.* **2021**, *155*, No. 184302.
(23) Wolk, A. B.; Leavitt, C. M.; Garand, E.; Johnson, M. A. Cryogenic Ion Chemistry and Spectroscopy. *Acc. Chem. Res.* **2014**, *47*, 202−210.
(24) Garand, E. Spectroscopy of Reactive Complexes and Solvated Clusters: A Bottom-Up Approach Using Cryogenic Ion Traps. *J. Phys. Chem. A* **2018**, *122*, 6479−6490.
(25) Okumura, M.; Yeh, L. I.; Myers, J. D.; Lee, Y. T. Infrared Spectra of the Cluster Ions $H_7O_3^+\cdot H_2$ and $H_9O_4^+\cdot H_2$. *J. Chem. Phys.* **1986**, *85*, 2328−2329.
(26) Nesbitt, D. J.; Field, R. W. Vibrational Energy Flow in Highly Excited Molecules: Role of Intramolecular Vibrational Redistribution. *J. Phys. Chem.* **1996**, *100*, 12735−12756.
(27) Tekavec, P. F.; Lott, G. A.; Marcus, A. H. Fluorescence-Detected Two-Dimensional Electronic Coherence Spectroscopy by Acousto-Optic Phase Modulation. *J. Chem. Phys.* **2007**, *127*, No. 214307.
(28) Tekavec, P. F.; Dyke, T. R.; Marcus, A. H. Wave Packet Interferometry and Quantum State Reconstruction by Acousto-Optic Phase Modulation. *J. Chem. Phys.* **2006**, *125*, No. 194303.
(29) Sanders, J. N.; Saikin, S. K.; Mostame, S.; Andrade, X.; Widom, J. R.; Marcus, A. H.; Aspuru-Guzik, A. Compressed Sensing for Multidimensional Spectroscopy Experiments. *J. Phys. Chem. Lett.* **2012**, *3*, 2697−2702.
(30) Maly, P.; Brixner, T. Fluorescence-Detected Pump-Probe Spectroscopy. *Angew. Chem., Int. Ed.* **2021**, *60*, 18867−18875.
(31) Roeding, S.; Brixner, T. Coherent Two-Dimensional Electronic Mass Spectrometry. *Nat. Commun.* **2018**, *9*, 2519.
(32) Bruder, L.; Bangert, U.; Binz, M.; Uhl, D.; Vexiau, R.; Bouloufa-Maafa, N.; Dulieu, O.; Stienkemeier, F. Coherent Multidimensional Spectroscopy of Dilute Gas-Phase Nanosystems. *Nat. Commun.* **2018**, *9*, 4823.
(33) Bruder, L.; Bangert, U.; Binz, M.; Uhl, D.; Stienkemeier, F. Coherent Multidimensional Spectroscopy in the Gas Phase. *J. Phys. B-Mol. Opt. Phys.* **2019**, *52*, No. 183501.
(34) Gutiérrez-Meza, E.; Malatesta, R.; Li, H.; Bargigia, I.; Srimath Kandada, A. R.; Valverde-Chávez, D. A.; Kim, S.-M.; Li, H.; Stingelin, N.; Tretiak, S.; Bittner, E. R.; Silva-Acuña, C. Frenkel Biexcitons in Hybrid HJ Photophysical Aggregates. *Sci. Adv.* **2021**, *7*, No. eabi5197.
(35) Jin, J.; Grellmann, M.; Asmis, K. R. Nuclear Quantum Dynamics on the Ground Electronic State of Neutral Silver Dimer $^{107}Ag^{109}Ag$ Probed by Femtosecond NeNePo Spectroscopy. *Phys. Chem. Chem. Phys.* **2023**, *25*, 24313−24320.
(36) Scherer, N. F.; Carlson, R. J.; Matro, A.; Du, M.; Ruggiero, A. J.; Romerorochin, V.; Cina, J. A.; Fleming, G. R.; Rice, S. A. Fluorescence-Detected Wave Packet Interferometry - Time Resolved Molecular-Spectroscopy with Sequences of Femtosecond Phase-Locked Pulses. *J. Chem. Phys.* **1991**, *95*, 1487−1511.
(37) Nikaido, M.; Mizuse, K.; Ohshima, Y. Torsional Wave-Packet Dynamics in 2-Fluorobiphenyl Investigated by State-Selective Ionization-Detected Impulsive Stimulated Raman Spectroscopy. *J. Phys. Chem. A* **2023**, *127*, 4964−4978.
(38) Nardin, G.; Autry, T. M.; Silverman, K. L.; Cundiff, S. T. Multidimensional Coherent Photocurrent Spectroscopy of a Semiconductor Nanostructure. *Opt. Express* **2013**, *21*, 28617−28627.
(39) Liebel, M.; Toninelli, C.; van Hulst, N. F. Room-Temperature Ultrafast Nonlinear Spectroscopy of a Single Molecule. *Nat. Photonics* **2018**, *12*, 45−49.
(40) Shim, S. H.; Strasfeld, D. B.; Ling, Y. L.; Zanni, M. T. Automated 2D IR Spectroscopy Using a Mid-IR Pulse Shaper and Application of this Technology to the Human Islet Amyloid Polypeptide. *Proc. Natl. Acad. Sci. U. S. A.* **2007**, *104*, 14197−14202.
(41) Yan, S.; Tan, H. S. Phase Cycling Schemes for Two-Dimensional Optical Spectroscopy with a Pump−Probe Beam Geometry. *Chem. Phys.* **2009**, *360*, 110−115.
(42) Chen, L.; Dean, J. L. S.; Fournier, J. A. Time-Domain Vibrational Action Spectroscopy of Cryogenically Cooled, Messenger-Tagged Ions Using Ultrafast IR Pulses. *J. Phys. Chem. A* **2021**, *125*, 10235−10244.
(43) Chen, L.; Ma, Z.; Fournier, J. A. Ultrafast Transient Vibrational Action Spectroscopy of Cryogenically Cooled Ions. *J. Chem. Phys.* **2023**, *159*, No. 041101.
(44) Golonzka, O.; Tokmakoff, A. Polarization-Selective Third-Order Spectroscopy of Coupled Vibronic States. *J. Chem. Phys.* **2001**, *115*, 297−309.
(45) King, J. T.; Baiz, C. R.; Kubarych, K. J. Solvent-Dependent Spectral Diffusion in a Hydrogen Bonded "Vibrational Aggregate. *J. Phys. Chem. A* **2010**, *114*, 10590−10604.
(46) Kiefer, L. M.; King, J. T.; Kubarych, K. J. Equilibrium Excited State Dynamics of a Photoactivated Catalyst Measured with Ultrafast Transient 2DIR. *J. Phys. Chem. A* **2014**, *118*, 9853−9860.
(47) Baiz, C. R.; McRobbie, P. L.; Anna, J. M.; Geva, E.; Kubarych, K. J. Two-Dimensional Infrared Spectroscopy of Metal Carbonyls. *Acc. Chem. Res.* **2009**, *42*, 1395−1404.
(48) Khalil, M.; Demirdoven, N.; Tokmakoff, A. Coherent 2D IR Spectroscopy: Molecular Structure and Dynamics in Solution. *J. Phys. Chem. A* **2003**, *107*, 5258−5279.
(49) De, A. K.; Monahan, D.; Dawlaty, J. M.; Fleming, G. R. Two-Dimensional Fluorescence-Detected Coherent Spectroscopy with Absolute Phasing by Confocal Imaging of a Dynamic Grating and 27-Step Phase-Cycling. *J. Chem. Phys.* **2014**, *140*, No. 194201.
(50) Mueller, S.; Brixner, T. Molecular Coherent Three-Quantum Two-Dimensional Fluorescence Spectroscopy. *J. Phys. Chem. Lett.* **2020**, *11*, 5139−5147.
(51) Mukamel, S. *Principles of Nonlinear Optical Spectroscopy*; Oxford University Press: New York, USA, 1995.
(52) Frisch, M. J.; Trucks, G. W.; Schlegel, H. B.; Scuseria, G. E.; Robb, M. A.; Cheeseman, J. R.; Scalmani, G.; Barone, V.; Mennucci, B.; Petersson, G. A.; Nakatsuji, H.; Caricato, M.; Li, X.; Hratchian, H. P.; Izmaylov, A. F.; Bloino, J.; Zheng, G.; Sonnenberg, J. L.; Hada, M.; Ehara, M.; Toyota, K.; Fukuda, R.; Hasegawa, J.; Ishida, M.; Nakajima, T.; Honda, Y.; Kitao, O.; Nakai, H.; Vreven, T.; Montgomery, J. A., Jr.; Peralta, J. E.; Ogliaro, F.; Bearpark, M. J.; Heyd, J.; Brothers, E. N.; Kudin, K. N.; Staroverov, V. N.; Kobayashi, R.; Normand, J.; Raghavachari, K.; Rendell, A. P.; Burant, J. C.; Iyengar, S. S.; Tomasi, J.; Cossi, M.; Rega, N.; Millam, N. J.; Klene, M.; Knox, J. E.; Cross, J. B.; Bakken, V.; Adamo, C.; Jaramillo, J.; Gomperts, R.; Stratmann, R. E.; Yazyev, O.; Austin, A. J.; Cammi, R.; Pomelli, C.; Ochterski, J. W.; Martin, R. L.; Morokuma, K.; Zakrzewski, V. G.; Voth, G. A.; Salvador, P.; Dannenberg, J. J.;

https://doi.org/10.1021/acs.jpclett.3c02661
J. Phys. Chem. Lett. 2023, 14, 9683−9689

Dapprich, S.; Daniels, A. D.; Farkas, Ö.; Foresman, J. B.; Ortiz, J. V.; Cioslowski, J.; Fox, D. J. *Gaussian 09*; Gaussian, Inc.: Wallingford, CT, USA, 2009.

(53) Hanes, A. T.; Grieco, C.; Lalisse, R. F.; Hadad, C. M.; Kohler, B. Vibrational Relaxation by Methylated Xanthines in Solution: Insights from 2D IR Spectroscopy and Calculations. *J. Chem. Phys.* **2023**, *158*, No. 044302.

(54) DeFlores, L. P.; Ganim, Z.; Nicodemus, R. A.; Tokmakoff, A. Amide I′−II′ 2D IR Spectroscopy Provides Enhanced Protein Secondary Structural Sensitivity. *J. Am. Chem. Soc.* **2009**, *131*, 3385−3391.

(55) Maekawa, H.; Ballano, G.; Toniolo, C.; Ge, N. H. Linear and Two-Dimensional Infrared Spectroscopic Study of the Amide I and II Modes in Fully Extended Peptide Chains. *J. Phys. Chem. B* **2011**, *115*, 5168−5182.

(56) Bloem, R.; Dijkstra, A. G.; Jansen, T. C.; Knoester, J. Simulation of Vibrational Energy Transfer in Two-Dimensional Infrared Spectroscopy of Amide I and Amide II Modes in Solution. *J. Chem. Phys.* **2008**, *129*, No. 055101.

(57) Roy, S.; Jansen, T. L. C.; Knoester, J. Structural Classification of the Amide I Sites of a β-Hairpin with Isotope Label 2DIR Spectroscopy. *Phys. Chem. Chem. Phys.* **2010**, *12*, 9347−9357.

(58) Backus, E. H. G.; Bloem, R.; Donaldson, P. M.; Ihalainen, J. A.; Pfister, R.; Paoli, B.; Caflisch, A.; Hamm, P. 2D-IR Study of a Photoswitchable Isotope-Labeled α-Helix. *J. Phys. Chem. B* **2010**, *114*, 3735−3740.

(59) Kratochvil, H. T.; Carr, J. K.; Matulef, K.; Annen, A. W.; Li, H.; Maj, M.; Ostmeyer, J.; Serrano, A. L.; Raghuraman, H.; Moran, S. D.; Skinner, J. L.; Perozo, E.; Roux, B.; Valiyaveetil, F. I.; Zanni, M. T. Instantaneous Ion Configurations in the K^+ Ion Channel Selectivity Filter Revealed by 2D IR Spectroscopy. *Science* **2016**, *353*, 1040−1044.

(60) Kwon, J. H.; Lee, M. J.; Song, G.; Tsuruta, K.; Ishiuchi, S.; Fujii, M.; Kang, H. Cryogenic Ion Spectroscopy of a Singly Protonated Peptide DYYVVR: Locating Phosphorylation Sites of a Kinase Domain. *J. Phys. Chem. Lett.* **2020**, *11*, 7103−7108.

(61) Rijs, A. M., Oomens, J., Eds.; *Gas-Phase IR Spectroscopy and Structure of Biological Molecules*; Springer International Publishing: Cham, Switzerland, 2015.

(62) Burke, N. L.; DeBlase, A. F.; Redwine, J. G.; Hopkins, J. R.; McLuckey, S. A.; Zwier, T. S. Gas-Phase Folding of a Prototypical Protonated Pentapeptide: Spectroscopic Evidence for Formation of a Charge-Stabilized β-Hairpin. *J. Am. Chem. Soc.* **2016**, *138*, 2849−2857.

(63) Dunbar, R. C.; Steill, J. D.; Polfer, N. C.; Oomens, J. Gas-Phase Infrared Spectroscopy of the Protonated Dipeptides H^+PheAla and H^+AlaPhe Compared to Condensed-Phase Results. *Int. J. Mass Spectrom.* **2009**, *283*, 77−84.

(64) Gorbachev, V.; Tsybizova, A.; Miloglyadova, L.; Chen, P. Increasing Complexity in a Conformer Space Step-by-Step: Weighing London Dispersion against Cation - π Interactions. *J. Am. Chem. Soc.* **2022**, *144*, 9007−9022.

(65) Voss, J. M.; Fischer, K. C.; Garand, E. Revealing the Structure of Isolated Peptides: IR-IR Predissociation Spectroscopy of Protonated Triglycine Isomers. *J. Mol. Spectrosc.* **2018**, *347*, 28−34.

(66) Rutherford, S. H.; Greetham, G. M.; Parker, A. W.; Nordon, A.; Baker, M. J.; Hunt, N. T. Measuring Proteins in H_2O Using 2D-IR Spectroscopy: Pre-Processing Steps and Applications toward a Protein Library. *J. Chem. Phys.* **2022**, *157*, No. 205102.

(67) Drozdov, A. N.; Grossfield, A.; Pappu, R. V. Role of Solvent in Determining Conformational Preferences of Alanine Dipeptide in Water. *J. Am. Chem. Soc.* **2004**, *126*, 2574−2581.

(68) Saparbaev, E.; Aladinskaia, V.; Zviagin, A.; Boyarkin, O. V. Microhydration of Biomolecules: Revealing the Native Structures by Cold Ion IR Spectroscopy. *J. Phys. Chem. Lett.* **2021**, *12*, 907−911.

(69) Marsh, B. M.; Voss, J. M.; Garand, E. A Dual Cryogenic Ion Trap Spectrometer for the Formation and Characterization of Solvated Ionic Clusters. *J. Chem. Phys.* **2015**, *143*, No. 204201.

(70) Racow, E. E.; Kreinbihl, J. J.; Cosby, A. G.; Yang, Y.; Pandey, A.; Boros, E.; Johnson, C. J. General Approach to Direct Measurement of the Hydration State of Coordination Complexes in the Gas Phase: Variable Temperature Mass Spectrometry. *J. Am. Chem. Soc.* **2019**, *141*, 14650−14660.

(71) Wyttenbach, T.; Bowers, M. T. Hydration of Biomolecules. *Chem. Phys. Lett.* **2009**, *480*, 1−16.

(72) Heiles, S.; Cooper, R. J.; DiTucci, M. J.; Williams, E. R. Hydration of Guanidinium Depends on its Local Environment. *Chem. Sci.* **2015**, *6*, 3420−3429.

(73) Nagornova, N. S.; Rizzo, T. R.; Boyarkin, O. V. Interplay of Intra- and Intermolecular H-Bonding in a Progressively Solvated Macrocyclic Peptide. *Science* **2012**, *336*, 320−323.

(74) Chen, L.; Ma, Z.; Fournier, J. A. Origins of the Diffuse Shared Proton Vibrational Signatures in Proton-Coupled Electron Transfer Model Dyad Complexes. *J. Chem. Phys.* **2022**, *157*, No. 154308.

(75) Craig, S. M.; Menges, F. S.; Duong, C. H.; Denton, J. K.; Madison, L. R.; McCoy, A. B.; Johnson, M. A. Hidden Role of Intermolecular Proton Transfer in the Anomalously Diffuse Vibrational Spectrum of a Trapped Hydronium Ion. *Proc. Natl. Acad. Sci. U. S. A.* **2017**, *114*, E4706−E4713.

(76) Wolke, C. T.; DeBlase, A. F.; Leavitt, C. M.; McCoy, A. B.; Johnson, M. A. Diffuse Vibrational Signature of a Single Proton Embedded in the Oxalate Scaffold, $HO_2CCO_2^-$. *J. Phys. Chem. A* **2015**, *119*, 13018−13024.

(77) Johnson, C. J.; Dzugan, L. C.; Wolk, A. B.; Leavitt, C. M.; Fournier, J. A.; McCoy, A. B.; Johnson, M. A. Microhydration of Contact Ion Pairs in $M^{2+}OH^-(H_2O)_{n=1-5}$ (M = Mg, Ca) Clusters: Spectral Manifestations of a Mobile Proton Defect in the First Hydration Shell. *J. Phys. Chem. A* **2014**, *118*, 7590−7597.

(78) Hamm, P.; Stock, G. Nonadiabatic Vibrational Dynamics in the $HCO_2^-\bullet H_2O$ Complex. *J. Chem. Phys.* **2015**, *143*, No. 134308.

(79) Florio, G. M.; Zwier, T. S.; Myshakin, E. M.; Jordan, K. D.; Sibert, E. L. Theoretical Modeling of the OH Stretch Infrared Spectrum of Carboxylic Acid Dimers Based on First-Principles Anharmonic Couplings. *J. Chem. Phys.* **2003**, *118*, 1735−1746.

(80) Yang, N.; Duong, C. H.; Kelleher, P. J.; Johnson, M. A. Capturing Intrinsic Site-Dependent Spectral Signatures and Lifetimes of Isolated OH Oscillators in Extended Water Networks. *Nat. Chem.* **2020**, *12*, 159−164.

(81) Zabuga, A. V.; Kamrath, M. Z.; Rizzo, T. R. Franck−Condon-like Progressions in Infrared Spectra of Biological Molecules. *J. Phys. Chem. A* **2015**, *119*, 10494−10501.

(82) Sibert, E. L. I.; Blodgett, K. N.; Zwier, T. S. Spectroscopic Manifestations of Indirect Vibrational State Mixing: Novel Anharmonic Effects on a Prereactive H Atom Transfer Surface. *J. Phys. Chem. A* **2021**, *125*, 7318−7330.

(83) Heine, N.; Kratz, E. G.; Bergmann, R.; Schofield, D. P.; Asmis, K. R.; Jordan, K. D.; McCoy, A. B. Vibrational Spectroscopy of the Water−Nitrate Complex in the O−H Stretching Region. *J. Phys. Chem. A* **2014**, *118*, 8188−8197.

https://doi.org/10.1021/acs.jpclett.3c02661
J. Phys. Chem. Lett. 2023, 14, 9683−9689